Received: 28 May 2021 | Revised: 23 August 2021 | Accepted: 22 September 2021

DOI: 10.1002/pat.5519

RESEARCH ARTICLE

polymers for advanced technologies WILEY

A liquid phosphorous flame retardant combined with expandable graphite or melamine in flexible polyurethane foam

Yin Yam Chan[1] | Chao Ma[2] | Feng Zhou[2] | Yuan Hu[2] | Bernhard Schartel[1]

[1]Bundesanstalt für Materialforschung und -prüfung (BAM), Berlin, Germany

[2]State Key Laboratory of Fire Science, University of Science and Technology of China, Hefei, China

Correspondence
Bernhard Schartel, Bundesanstalt für Materialforschung und -prüfung (BAM), Unter den Eichen 87, 12205 Berlin, Germany.
Email: bernhard.schartel@bam.de

Funding information
Deutsche Forschungsgemeinschaft, Grant/Award Number: Scha 730/19-1; National Natural Science Foundation of China, Grant/Award Number: 51761135113

Abstract

A systematic series of flexible polyurethane foams (FPUF) with different concentrations of flame retardants, bis([dimethoxyphosphoryl]methyl) phenyl phosphate (BDMPP), and melamine (MA) or expandable graphite (EG) was prepared. The mechanical properties of the FPUFs were evaluated by a universal testing machine. The pyrolysis behaviors and the evolved gas analysis were done by thermogravimetric analysis (TGA) and TGA coupled with Fourier-transform infrared (TG-FTIR), respectively. The fire behaviors were studied by limiting oxygen index (LOI), UL 94 test for horizontal burning of cellular materials (UL 94 HBF), and cone calorimeter measurement. Scanning electronic microscopy (SEM) was used to examine the cellular structure's morphology and the postfire char residue of the FPUFs. LOI and UL 94 HBF tests of all the flame retarded samples show improved flame retardancy. BDMPP plays an essential role in the gas phase because it significantly reduces the effective heat of combustion (EHC). This study highlights the synergistic effect caused by the combination of BDMPP and EG. The measured char yield from TGA is greater than the sum of individual effects. No dripping phenomenon occurs during burning for FPUF-BDMPP-EGs, as demonstrated by the result of the UL 94 HBF test. EG performs excellently on smoke suppression during burning, as evident in the result of the cone calorimeter test. MA reduces the peak heat release rate (pHRR) significantly. The synergistic effect of the combination of BDMPP and EG as well as MA offers an approach to enhance flame retardancy and smoke suppression.

KEYWORDS
bis([dimethoxyphosphoryl]methyl) phenyl phosphate, expandable graphite, flexible polyurethane foam, melamine, phosphorous flame retardant

1 | INTRODUCTION

Generally, polyurethanes (PU) are a class of copolymers composed of soft and hard segments. Usually, the soft segment is a polyester or a polyether polyol, whereas the hard segment is composed of isocyanate and maybe chain extender if needed.[1]The soft segment determines elasticity, while the hard segment provides strength and rigidity. PU with desired physical and mechanical properties can be produced by altering the ratio of the soft segment to the hard segment. For the past several decades, PU has been used frequently because of its wide range of applications in products such as foams, elastomers, adhesives, paints, and coatings. The PU foams are usually classified into rigid, semi-rigid, and flexible types, depending primarily on the density and degree of openness of the cells. Closed-cell rigid PU foam is used mainly for

thermal insulation in buildings and refrigerators. Open-cell flexible PU foam (FPUF) is used as a cushion material in furniture, vehicles, and packaging. It is easy to ignite PU foams readily by a small flame source, and they burn quickly with a high rate of heat release because of their cellular structure, low density, and high hydrocarbon content.[2–5]To reduce the possibility of fire, commercial additive-type flame retardants available on the market are simply physically mixed with the polymer matrix. Metal hydroxides, halogenated compounds, phosphorous compounds, melamine cyanurate, and intumescent products are commonly used as flame retardants in polymers.[6]The concerns regarding health and environmental problems caused by halogenated flame retardants aroused interest among scientists in developing non-halogenated flame retardants. Interestingly, incorporating more than one type of flame retardant into the polymer matrix may bring a synergistic effect to flame retardancy.[7,8]A synergistic effect means that the overall flame retardancy is even better than the superposition of the individual component's effects. Wilke et al. studied the synergetic effect between phosphorus and expandable graphite (EG) in thermoplastic styrene-ethylene-butylene-styrene elastomers.[9]Rao et al. found that EG and phosphorus contributed to the compactness of char residue in FPUF.[10]This is due to the gluing effect on to the fluffy expanded graphite exerted by the phosphorous compound. They concluded that the intensity of synergism, which provides better flame retardancy to the material, increased significantly when the proper ratio of EG to phosphorus was applied. Feng et al. explored the synergistic effect between phosphorus and EG as well.[11]They showed that the system remarkably increased residual char yield and intensely reduced the fire parameters compared to the one using a single flame retardant. Synergistic action is apparent in the polymer matrix with phosphorus and nitrogen compounds. Yuan et al. synthesized phosphorous and melamine-derived polyol for rigid polyurethane foam and found out that the appropriate ratio between these components greatly improved the material's fire performance.[12] Phosphorus-nitrogen synergism in cotton cellulose was a focus of the work by Gaan and his coworkers.[13]They proposed that the formation of a protective layer during the burning process was an observable effective synergism between phosphorus and nitrogen. The voluminous protective layer acted as a shield to prevent further burning of the underlying materials. By taking advantage of synergism, a smaller quantity of flame retardants can be used to maintain the physical and mechanical properties of the material. Among different phosphorous flame retardants, dimethyl methylphosphonate (DMMP) is an effective flame retardant because it contains a rather high content of phosphorus (25 wt%) compared to other phosphorous flame retardants, such as 9,10-dihydro-9-oxa-10-phosphaphenanthrene-10-oxide, triphenyl phosphate, triethyl phosphate, and aluminum diethylphosphinate. In this work, a liquid phosphorous flame retardant, bis([dimethoxyphosphoryl]methyl) phenyl phosphate (BDMPP), was combined with two commercial flame retardants, melamine (MA) and EG in FPUF. Zhou et al. proposed and compared BDMPP with dimethyl methylphosphonate (DMMP) in terms of fire properties; they found that BDMPP is more advantageous to flame retardancy than DMPP.[14] BDMPP still contains a very high phosphorus content (22 wt%). BDMPP contains two kinds of phosphorus, phosphonate, and phosphate, since it is synthesized from dimethyl (hydroxymethyl) phosphonate and phenyl dichlorophosphate. The presence of aromatic rings in BDMPP contributed to a better charring effect and an increased char yield in the condensed phase during burning. The molecular weight of BDMPP is higher than that of DMMP. Hence, BDMPP provided superior retainability to inhibit migration and volatilization. The current work focusses on the flame retardancy and fire performance of FPUF incorporated with BDMPP, MA, and EG.

2 | EXPERIMENTAL

2.1 | Materials

The chemicals used in the foaming formulation are described in Table 1. The materials listed in Table 1, except deionized water, were provided by Jiangsu Lvyuan New Material Co., Ltd. (Jiangsu, China).

For the flame retardants, EG flakes with an expansion ratio of 150–200 and particle size of 30–50 μm were supplied by Qingdao Xingyuan Colloidal Graphite Co., Ltd. (Qingdao, China). MA was purchased from Anhui Jinhe Chemical Co., Ltd (Shanghai, China). BDMPP was prepared by the State Key Laboratory of Fire Science, the University of Science and Technology of China, following the procedures described in Reference 14. The attention of readers interested in corresponding information on BDMPP is also turned to the original paper published on its synthesis.[14]

A set of foam samples were prepared at the State Key Laboratory of Fire Science, University of Science and Technology of China. Three additive-type flame retardants were used in the FPUF. One of the flame retardants is a liquid phosphorous flame retardant, shown in Figure 1, called bis([dimethoxyphosphoryl]methyl) phenyl phosphate

TABLE 1 Foaming formulation of flexible polyurethane foam

	Material	Weight (g)
Component A	Polyether polyol (330, hydroxyl value = 56 mg KOH/g, number average molecular weight = 3000 g/mol, average functionality =3)	62.5
	Grafted polyether polyol (2045, prepared by the in situ polymerization of acrylonitrile and styrene in a polyether polyol, hydroxyl value = 20 mg KOH/g, number average molecular weight = 8400 g/mol, functionality = 3)	20.83
	Silicone oil	0.92
	Stannous octoate	0.15
	Triethylenediamine (A33, 33%)	0.23
	Dichloromethane	2.92
	Deionized water	2.67
Component B	Toluene diisocyanate (TDI 80/20, 80:20 mixture of 2,4-toluene diisocyanate and 2,6-toluene diisocyanate)	38.33

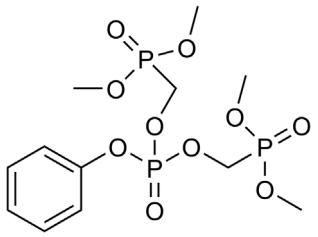

FIGURE 1 Bis([dimethoxyphosphoryl]methyl) phenyl phosphate (BDMPP)

(BDMPP). The rest are all commercial flame retardants, MA and EG. Each sample, except the reference sample FPUF, contains 20-phr of the polyether polyol and the grafted polyether polyol blended with a sole flame retardant or adual flame retardant.Table 2 shows the type and amount of flame retardants used in each sample. The additive flame retardants were weighted based on parts per hundred of the sum of polyether polyol and grafted polyether polyol.

TABLE 2 Content of flame retardants in the samples

Sample	Flame retardants (in phr[a])
FPUF	–
FPUF-20BDMPP	20-phr BDMPP
FPUF-20MA	20-phr MA
FPUF-20EG	20-phr EG
FPUF-5BDMPP-15MA	5-phr BDMPP and 15-phr MA
FPUF-10BDMPP-10MA	10-phr BDMPP and 10-phr MA
FPUF-15BDMPP-5MA	15-phr BDMPP and 5-phr MA
FPUF-5BDMPP-15EG	5-phr BDMPP and 15-phr EG
FPUF-10BDMPP-10EG	10-phr BDMPP and 10-phr EG
FPUF-15BDMPP-5EG	15-phr BDMPP and 5-phr EG

[a]phr, Parts per hundred of the sum of polyether polyol and grafted polyether polyol.

2.2 | Sample preparation

The preparation of FPUF was conducted by mixing component A and component B using the one-pot method. The foams were prepared at 60°C for 20 min in a temperature controlled closed mold 200 × 200 × 100 mm (length×width×thickness) in size. First, component A was stirred uniformly in a disposable polypropylene cup by a high-speed stirrer for 3 min. Afterward, component B was mixed with the blended component A for few seconds under a high stirring rate. Then the mixture was discharged into the mold. The foam was cured for 24 h in an oven at 80°C to complete the polymerization.

2.3 | Measurements and characterization

2.3.1 | Morphological characterization

The micrographs of the foams and their char residues were examined using a scanning electron microscope (SEM) Zeiss EVO 10 (Oberkochen, Germany). The acceleration voltage was set to 10 kV. The specimens were sputter-coated with 15 nm of gold to reduce the chances of electrostatic charging. Only the foam structure at the surface, the direct interface with the mold, shows a skin accompanied with a thin layer of smaller cell size and higher density. We prepared and investigated only specimens cut out from the inner homogenous part of the foams.

2.3.2 | Physical and mechanical properties measurements

The apparent density of the specimen was measured according to ISO 845. A Universal Testing Machine Zwick Z010 (Ulm, Germany) was used to evaluate the tensile strength, elongation at break, and compression strength. A load cell with 500 N was used, the speed of the power-actuated grip was 500 mm/min for the tensile test. The strain rate was 100 mm/min for the compression test. The tensile strength and elongation at break were measured using specimens with a thickness of 10 mm cut as test piece type 1A following ISO 1798, while the compressive strength was measured according to ISO 3386-1. The specimen size for determining the compression was 40 × 30 × 10 mm (length×width×thickness). 3 cycles of compression were performed for the compression test. Four and three test specimens were measured for each material in the tensile test and the compression test, respectively.

2.3.3 | Pyrolysis: Mass loss and evolved gases

Thermogravimetric analysis (TGA) records the change in the mass of a sample as a function of time under a nitrogen atmosphere using a TG 209 F1 Iris from Netzsch Instruments (Selb, Germany), thereby determining the thermal decomposition behavior of the samples. The alumina crucible with 10 mg of the powdered sample was then put on the thermo-microbalance of the TGA device. The samples were subjected to a heating program under a constant nitrogen gas flow of 30 ml/min at a steady heating rate of 10 K/min. Simultaneously, TGA coupled with Fourier transform infrared spectroscopy (FTIR), Brucker Tensor 27 FT-IR (Ettlingen, Germany) analyzes the gaseous pyrolysis products evolved from the specimens in the furnace.

2.3.4 | Fire behavior

Before the measurements, all test specimens were stored at 23°C and 50% relative humidity for a minimum of 48 h. The limiting oxygen index (LOI) of the specimens 150 × 10 × 10 mm (length×width×thickness) in size was determined at room temperature according to ISO 4589-2. The fire behavior was analyzed using a cone calorimeter from Fire Testing Technology Limited (West Sussex, United Kingdom), and the test was carried out in accordance with ISO 5660. The specimen for the

cone calorimeter is 100 × 100 × 50 mm (length×width×thickness) in size. The specimen placed in an aluminum foil container was exposed in the horizontal orientation to a radiative heat flux of 25 kW m^{-2} with a distance of 25 mm between the cone heater and the surface of the specimen. All materials showed and impressive repeatability and thus were only measured twice in the cone calorimeter. UL 94 HBF is used to measure the burning rate and evaluate the tendency of the materials to either extinguish or spread the flame when the specimen has been ignited. It was performed to determine the horizontal burning characteristics following ISO 9772 with a specimen size of 150 × 50 × 10 mm (length×width×thickness). The number of specimens for LOI and UL 94 were according to the standards.

3 | RESULTS AND DISCUSSION

3.1 | Morphological characterization and mechanical properties measurements

The morphology is a critical factor that influences the physical and mechanical properties of FPUF. A scanning electron microscope (SEM) was used to observe the morphology of foams, and the SEM images are displayed in Figure 2. All foams show a semi-open cell structure. The FPUF in Figure 2A has smoother edges on the blow-holes, uniform cell size, and even cell distribution. Generally, high loading of additive-type flame retardants must be incorporated into the polymer matrix for better flame retardancy. Therefore, the high content of additive-type flame retardants is often detrimental to the mechanical properties, as they function mainly as a nucleating agent. The SEM images show the influence of flame retardants on cellular structures. FPUF-20BDMPP, and FPUF-20MA in Figure 2B,C, respectively, show a similar structure with cells slightly larger than in FPUF. The SEM images of FPUF-20EG and FPUF-BDMPP-EGs show less continuous and less regular spherical cell structure. This phenomenon was attributed to nucleation triggered by EG particles in the polymer matrix.[15–16]EG is a kind of solid particle that affects bubble nucleation and bubble growth in the foaming process, thereby damaging the foam's structure to some extent. Especially for FPUF-10BDMPP-10EG shown in Figure 2I, the struts are somewhat thicker, and the cellular structure is somewhat less complete than the others.

Density is a major parameter affecting foam flexibility and support. The apparent density of the flame retardant samples shown in Table 3

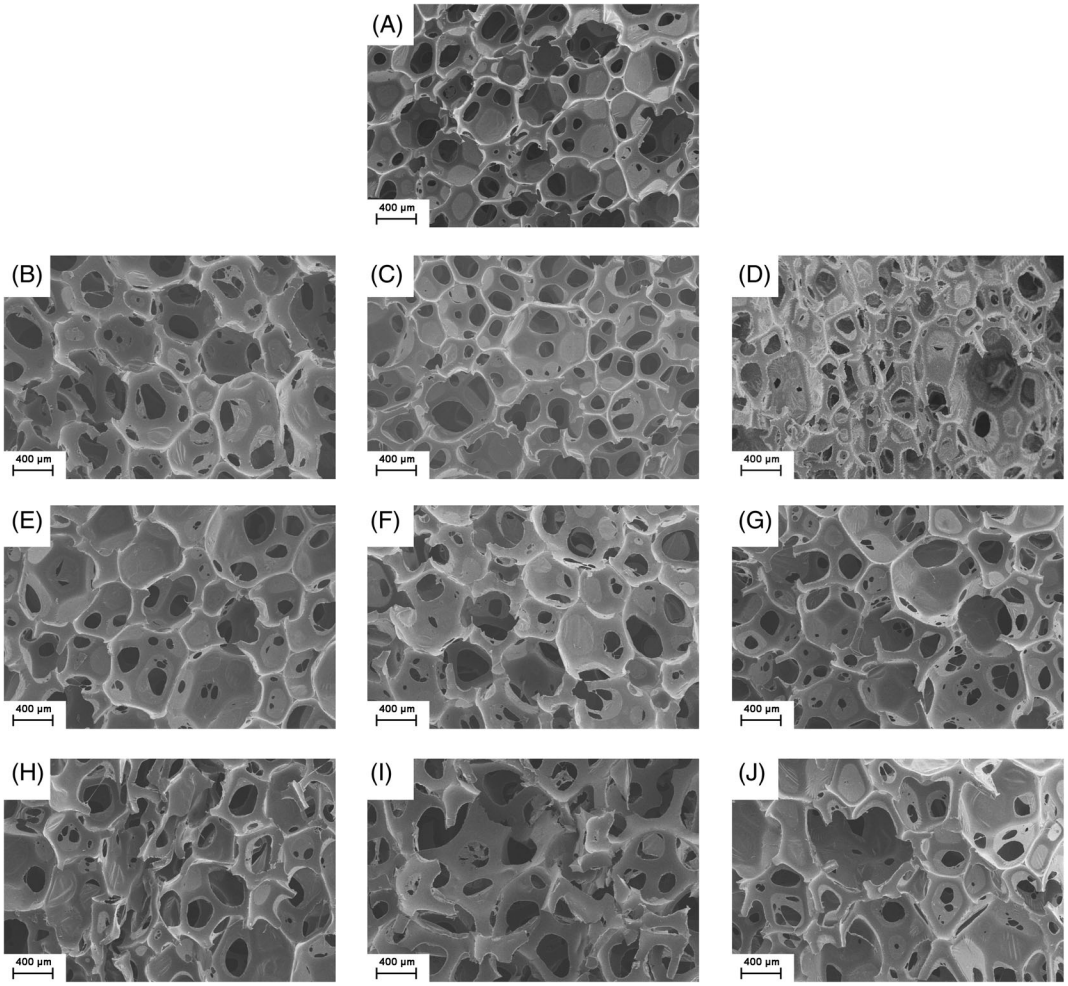

FIGURE 2 SEM images of (A) FPUF, (B) FPUF-20BDMPP, (C) FPUF-20MA, (D) FPUF-20EG, (E) FPUF-5BDMPP-15MA, (F) FPUF-10BDMPP-10MA, (G) FPUF-15BDMPP-5MA, (H) FPUF-5BDMPP-15EG, (I) FPUF-10BDMPP-10EG, (J) FPUF-15BDMPP-5EG

TABLE 3 Mechanical test results of the samples

Sample	Tensile strength (kPa)	Elongation at break (%)	Compression stress valueat 40% compression (CV_{40}) (kPa)	Apparent density (kg m^{-3})
FPUF	126 ± 13	138 ± 9	6.61 ± 0.13	34.2 ± 0.4
FPUF-20BDMPP	140 ± 16	140 ± 16	6.37 ± 0.21	40.1 ± 2.2
FPUF-20MA	102 ± 13	91 ± 15	6.34 ± 0.12	34.4 ± 0.7
FPUF-20EG	156 ± 9	111 ± 11	6.08 ± 0.20	35.9 ± 2.3
FPUF-5BDMPP-15MA	94 ± 11	87 ± 16	6.67 ± 0.87	37.9 ± 2.3
FPUF-10BDMPP-10MA	93 ± 10	96 ± 11	5.30 ± 0.29	40.2 ± 0.5
FPUF-15BDMPP-5MA	54 ± 9	104 ± 14	1.99 ± 0.19	33.8 ± 0.7
FPUF-5BDMPP-15EG	139 ± 4	151 ± 4	5.98 ± 0.75	38.9 ± 3.4
FPUF-10BDMPP-10EG	112 ± 4	145 ± 8	4.22 ± 0.09	42.0 ± 8.8
FPUF-15BDMPP-5EG	54 ± 14	83 ± 17	2.84 ± 0.53	33.7 ± 0.9

ranges from 33.7 to 42 kg m^{-3}, which is comparable to the FPUF. FPUF-20BDMPP exhibits the highest density among the FPUFs with other single flame retardants. For the FPUFs containing two flame retardants, FPUF-10BDMPP-10EG shows the highest density. FPUF-15BDMPP-5MA and FPUF-15BDMPP-5EG show the lowest density. Additive flame retardants often show an adverse effect on the density of foams. Here in this study, no significant change occurred in the density of the foams.

The mechanical properties of FPUFs were evaluated by measuring their tensile strength, elongation at break, and compression. The data are listed in Table 3. Apart from foam density, the additives themselves influence the mechanical properties. The value for the tensile strength of FPUF-20EG is the highest of all the samples, which means the EG improved the tensile strength of FPUF. This effect of EG is also obvious in FPUF-5BDMPP-15EG and FPUF-10BDMPP-10EG. Among the FPUFs with 20-phr of a single flame retardant, FPUF-20MA has the lowest tensile strength and elongation at break, but still has good mechanical properties. The melamine particles weakened the structure by stiffening the cellular network.[17]This effect of MA can also be observed in FPUF-5BDMPP-15MA and FPUF-10BDMPP-10MA. For the FPUFs with the combination of two flame retardants, the incorporation of 15-phr BDMPP with either 5-phr MA or 5-phr EG in FPUF significantly reduces tensile strength and compression stress/straincharacteristic at 40% compression (CV_{40}) because of the lower density and detrimental effects to the mechanical properties caused by the two flame retardants. Apart from FPUF-15BDMPP-5MA and FPUF-15BDMPP-5EG, all the other seven foams showed very similar mechanical properties compared to FPUF. Thus, the mechanical properties of the foam depend on the amount and the type of flame retardant added.

3.2 | Pyrolysis: Mass loss

The thermal decomposition behavior of the FPUFs was investigated. The pyrolysis of organic content typically generates volatile products and leaves mostly carbonaceous char as residue. TGA measured the mass loss of the FPUFs during the pyrolysis process under a nitrogen atmosphere. Figure 3 shows the mass and the first derivative of mass loss (DTG) curves, and Table 4 records the selected data. $T_{5\%}$ and T_{max} are the temperatures where 5-wt% mass loss and maximum mass loss occurred, respectively. All FPUFs went through two distinguishable decomposition steps based on the chemical structure of the FPUF.[18] There is no additional separated minor decomposition step happening at lower temperatures, an early decomposition or release of BDMMP were ruled out. The first weight loss is related to the urethane bond's cleavage, while the second step is attributed to the decomposition of the hydrocarbon chains.[19,20] FUPF-20BDMPP shows the lowest $T_{5\%}$ at approximately 220°C, which is due to the interaction between polyurethane decomposition and the phosphorous compounds of BDMPP decomposition.[2,21] Among the FPUFs incorporated with a sole retardant, 8.2 and 7.5-wt% of char yield were measured for FPUF-20BDMPP and FPUF-20EG, respectively, while there was no significant degree of charring for FPUF-20MA. It is evident that BDMPP and EG worked in the condensed phase, while MA did not. Phosphorous compounds enhanced carbonization, while EG yielded intumescence and remained in the crucible because EG cannot evaporate during thermal decomposition.[22,23] The amount of char residue of all FPUF-BDMPP-EGs is greater than that of either FPUF-20BDMPP or FPUF-20EG. The synergistic effect caused by the combination of BDMPP and EG was attributed to the phosphorous flame retardant, which generates char-forming catalysts, increasing the char yield during thermal decomposition.[10,24] FPUF-20EG shifted the first and second decomposition steps towards the highest temperature (T_{max} #1 = 313°C and T_{max} #2 = 383°C) among all the samples, which indicates that 20-phr EG enhanced the thermal stability of the system.

3.3 | Pyrolysis: Evolved gas analysis

The evolved gaseous products during thermal decomposition under nitrogen atmosphere were determined using TG-FTIR. The TG-FTIR were performed to characterize how the single flame retardant work,

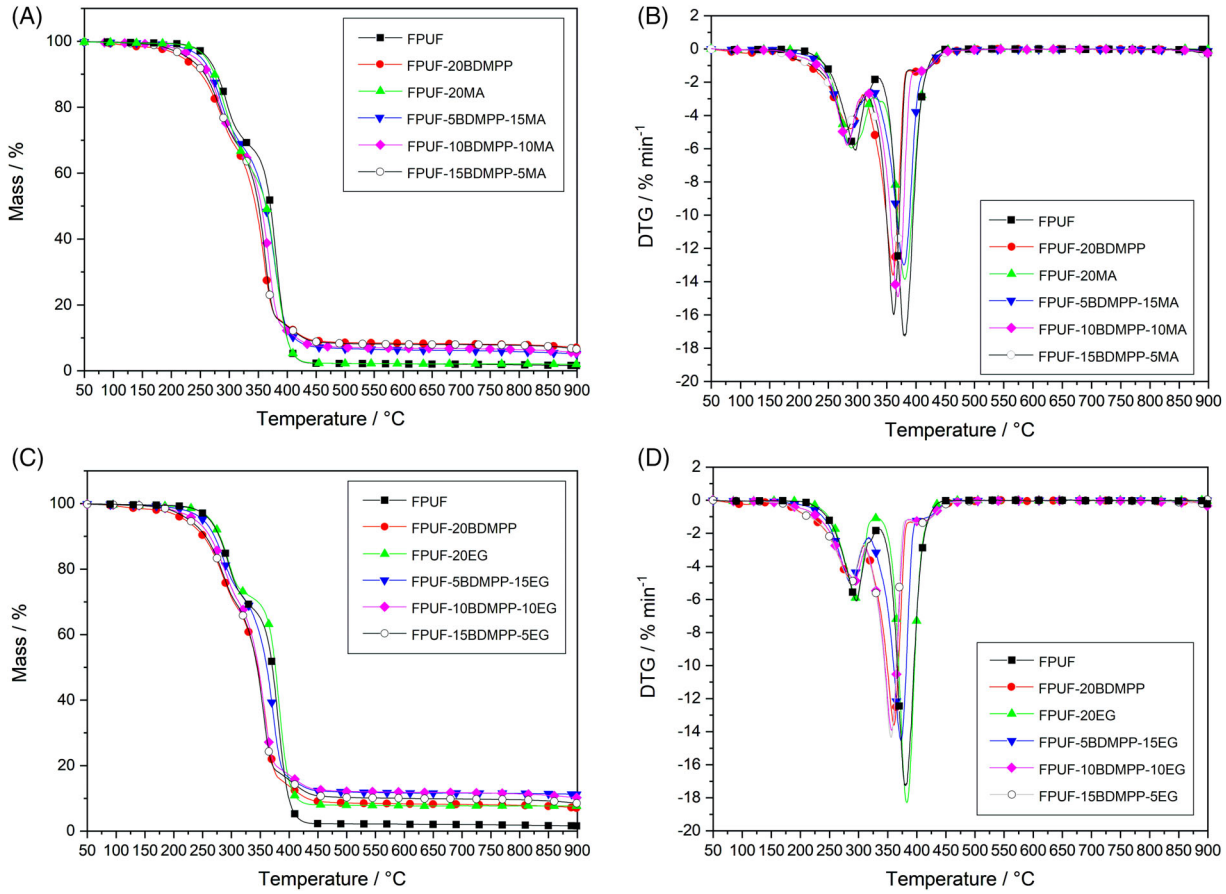

FIGURE 3 Thermogravimetry-(A) mass curves and (B) DTG curves of FPUF-BDMPP-MAs; (C) mass curves and (D) DTG curves of FPUF-BDMPP-EGs

TABLE 4 Selected thermogravimetry results obtained from the mass and DTG curves of FPUFs

Material	$T_{5\%}$ (°C)	T_{max} #1 (°C)	T_{max} #2 (C)	Mass change #1 (wt%)	Mass change #2 (wt%)	Residue at 700°C (wt%)
FPUF	263	297	380	31.2	65.7	1.6
FPUF-20BDMPP	220	288	360	29.3	60.5	8.2
FPUF-20MA	260	290	381	34.7	62.7	2.0
FPUF-20EG	265	313	383	27.4	64.4	7.5
FPUF-5BDMPP-15MA	252	284	379	32.5	62.2	5.7
FPUF-10BDMPP-10MA	242	282	369	31.6	61.0	6.9
FPUF-15BDMPP-5MA	229	281	362	30.2	60.8	7.9
FPUF-5BDMPP-15EG	251	287	372	27.1	60.4	11.8
FPUF-10BDMPP-10EG	238	295	356	29.3	59.2	11.6
FPUF-15BDMPP-5EG	228	289	356	29.3	59.9	9.9

Abbreviations: $T_{5\%}$, the temperature at 5% mass loss; T_{max} #1, the first maximum mass loss rate; T_{max} #2, The second maximum mass loss rate.

particular which one is releasing phosphorus in the gas phase. Apart from that, the limited change in TG curves yields evolved gas analysis being of minor importance for understanding the fire behavior. As shown in Figure 4A, some characteristic bands were detected during the pyrolysis process. The noisy signals in the ranges of 2150–1250 and 4000–3400 cm^{-1} are related to the water vapor produced during thermal decomposition. The peaks of CO_2 (2360 and 670 cm^{-1}) were observed.[25] The peak at 2276 cm^{-1} is attributed to the stretching vibration of N═C═O. From about 340°C, the transmittance intensity at 2276 cm^{-1} of —NCO disappeared. This indicates that N═C═O is the main product generated in the first stage of decomposition.[26,27] The broad peaks at 3000–2850 cm^{-1} at 340 to 440°C are attributed to hydrocarbons.[28] Therefore, the major products in the second stage are hydrocarbons. The peaks at 1734 and 1363 cm^{-1} correspond to

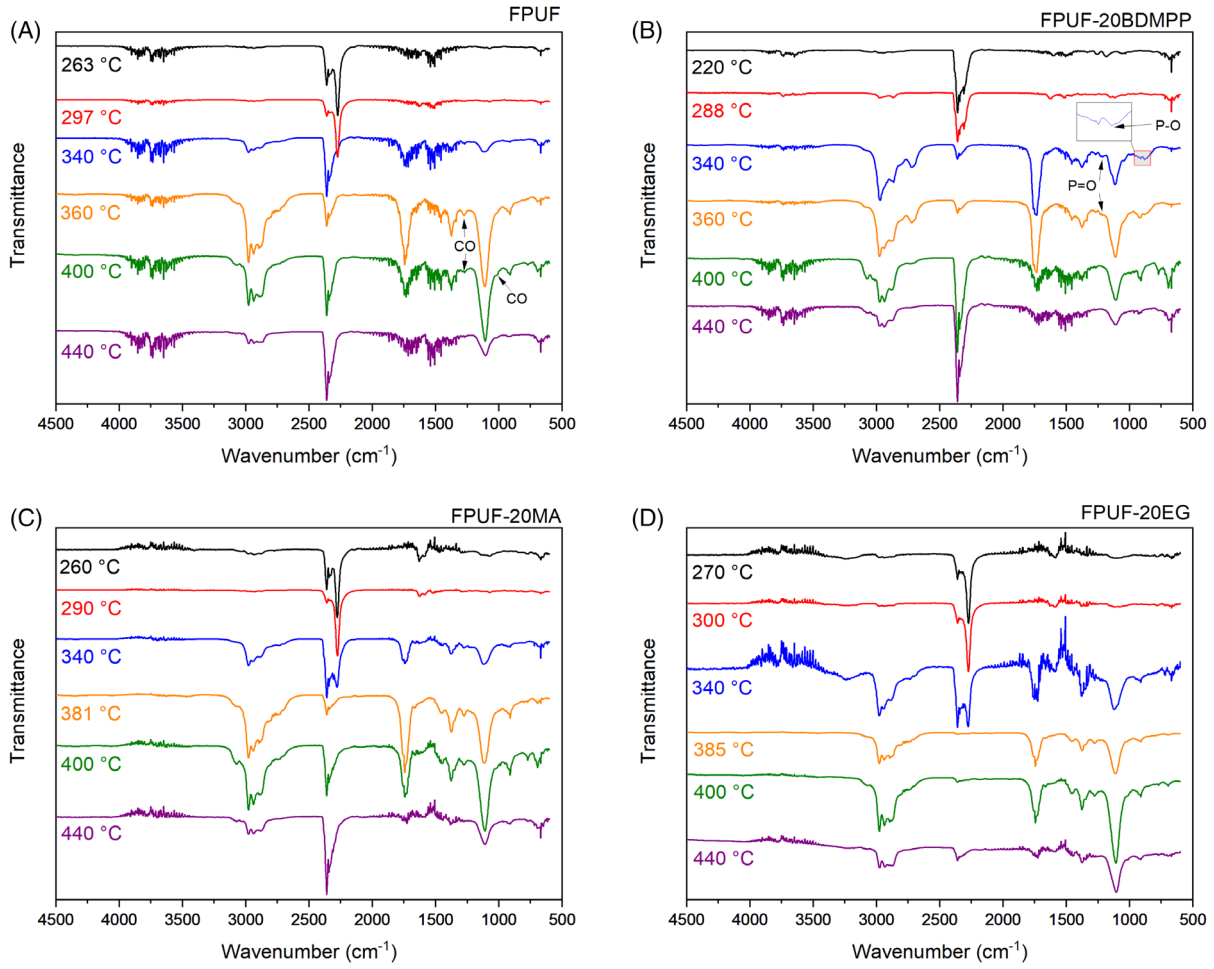

FIGURE 4 TG-FTIR spectra of the gas phase in the thermal degradation of (A) FPUF, (B) FPUF-20BDMPP, (C) FPUF-20MA, and (D) FPUF-20EG at different pyrolysis temperatures

the stretching vibration of the carbonyl compound.[28] The peaks at 1272 and 1110 cm^{-1} are attributed to C—O stretching. Figure 4B shows that the peaks at 1218 and 880 cm^{-1} are attributed to P═O and P—O, respectively.[26] The phosphorous moieties are released mainly during the second stage of decomposition. As a result, the fragments composed of phosphorus in the gas phase provide a radical quenching effect during combustion. As shown in Figure 4C, the peak at 1660 cm^{-1} is attributed to the triazine ring of melamine.[29] The nitrogen from MA produced by combustion acts as an inert diluent, diluting the fuel gases. There are smaller peaks in Figure 4D at 2400–2300 cm^{-1} and 670 cm^{-1} related to CO_2 in the range from 383 to 400°C. This is probably due to the presence of EG, which may produce more stable char residue to change the CO_2 release. In conclusion, the results agree with the decomposition pathway of FPUF described in the literature.[30]

3.4 | Fire behavior: Reaction to the small flame

The limiting oxygen index (LOI) is a measure of the minimum percentage of oxygen in a mixture of oxygen and nitrogen gases required to support the combustion of materials in a candle-like setup. Table 5 lists the LOI value of the samples. All the FPUFs with flame retardants show improvement in the LOI values. The improvements are somewhat limited prospecting for further development. Nevertheless, considering that foams were investigated and there is no significant difference in morphology and density the increase in LOI is assessed to be meaningful. When 20-phr BDMPP, MA, or EG was added to FPUF, the LOI values increase, and their values are very similar: 20.0, 20.4, and 20.8 vol%, respectively. However, FPUFs with a single flame retardant exhibit typical LOI values of foams, limiting flame retardancy to FPUF. The LOI value of FPUFs containing different proportions of BDMPP and MA remains the same as those with single flame retardants. Nevertheless, it is notable that FPUF-5BDMPP-15EG achieved the highest LOI value among all the samples. With an increase of 3.6 to 22.2 vol%. FPUF-10BDMPP-10EG shows the second highest LOI value, 21.8 vol%. The higher EG content in FPUF-BDMPP-EGs provides the polymer with better fire protection, as observed in this case. Therefore, the optimal ratio of BDMPP to EG in FPUF-BDMPP-EGs that produces the greatest synergy is 1: 3.[31]

The results in Table 6 show that all the modified samples exhibit different degrees of improvement to flame retardancy in the UL

94 HBF test as compared to FPUF. FPUF burned entirely with the fastest burning rate and significant dripping behavior. The burning rate of all the foams with 20-phr of either a single or dual flame retardant(s) decreased compared to that of FPUF (120 mm/min). The EG contributed effectively to slowing down the burning rate. Due to the formation of a dense carbon layer, all samples with EG completely stopped the melt dripping. The expanded graphite served as a carrier to retain the polymer melt. Compared to FPUF-20EG, FPUF-5BDMPP-15EG exhibited a lower burning rate and exhibited self-extinguishing behavior, even though less EG was added. This is because the synergistic effect was exerted by BDMPP and EG. The gluing effect of BDMPP strengthened the integrality and continuity of the EG char layer.[32,33]The burning rate of FPUF-5BDMPP-15MA was lower than that of FPUF-20BDMPP and FPUF-20MA. This indicates that 5-phr of BDMPP with either 15-phr of EG or 15-phr MA in the FPUF is enough to yield a remarkable synergistic effect in flame retardancy.

3.5 | Fire behavior: Cone calorimeter

A cone calorimeter is used to evaluate a comprehensive set of fire properties such as time of ignition (t_{ig}), peak heat release rate (PHRR), total heat release (THR), average effective heat of combustion (EHC), residue, total smoke released (TSR) and the maximum average rate of heat emission (MARHE) in the fire scenarios of developing fires. Heat release rate (HRR) and THR curves of FPUF-BDMPP-MAs and FPUF-BDMPP-EGs are displayed in Figure 5. The measured data are presented in Table 7.

Typically, the HRR curve of FPUF consists of the two peaks associated with two-step decomposition, which is concluded from the result of TGA in accordance with the literature.[34,35]The first decomposition step corresponds to the breaking of the urethane bond in PU, while the soft segment dominates the second step. The HRR curve of FPUF shows two peaks of heat release rate, where the second peak (pHRR at 503 kW m^{-2}) is higher than that of the first peak (pHRR at 294 kW m^{-2}). The t_{ig} is usually very short because of the low heat conductivity of FPUFs. At the first peak, the material was ignited, and the cellular structure started to collapse, thus producing volatile and liquid fragments. These liquid fragments produced more heat by oxidation and quickly developed a feedback loop. Subsequently, this feedback loop at the second peak with a high HRR formed a pool fire, and the sample burned intensively. After that, as the fuel was consumed, HRR dropped rapidly until the flame went out.[36,37] Figure 5 (A1) shows that the HRR curves of the FPUFs with flame retardant(s) are similar to those of FPUF, with two explicit HRR peaks and the second peak higher than the first.

The EHC monitored in the cone calorimeter is a product of the effective heat of combustion of the volatiles and the combustion efficiency of the flame. The fuel dilution, reducing the effective heat of combustion of the volatiles, and flame inhibition, reducing mainly the combustion efficiency in the flame, reduce the EHC. Therefore, EHC is an important parameter to measure the activity of flame retardants in the gas phase. A reduction in EHC is observed for all flame retarded samples in Table 7, indicating that all flame retardants exerted different degrees of flame retardant effects in the gas phase. Among the FPUFs containing a single flame retardant, the best result in terms of EHC was achieved by FPUF-20BDMPP (22 MJ kg^{-1}). The EHC of FPUF-20BDMPP reduces by more than 14% when compared to the that of FPUF. This showed that the BDMPP plays an important role as a flame retardant through flame inhibition in the gas phase.[38] As

TABLE 5 LOI measurement

Sample	LOI/vol%
FPUF	18.6 ± 0.2
FPUF-20BDMPP	20.0 ± 0.2
FPUF-20MA	20.4 ± 0.1
FPUF-20EG	20.8 ± 0.2
FPUF-5BDMPP-15MA	20.0 ± 0.2
FPUF-10BDMPP-10MA	20.2 ± 0.1
FPUF-15BDMPP-5MA	20.6 ± 0.1
FPUF-5BDMPP-15EG	22.2 ± 0.2
FPUF-10BDMPP-10EG	21.8 ± 0.2
FPUF-15BDMPP-5EG	20.6 ± 0.1

TABLE 6 Result of UL 94 horizontal burning tests

Material	Burning time (s)	Distance burned (mm)	Burning drops	Burning rate (mm/min)
FPUF	50	100	Yes	120
FPUF-20BDMPP	63	100	Yes	95
FPUF-20MA	108	100	Yes	56
FPUF-20EG	46	15	No	20
FPUF-5BDMPP-15MA	131	100	Yes	46
FPUF-10BDMPP-10MA	69	100	Yes	87
FPUF-15BDMPP-5MA	70	100	Yes	86
FPUF-5BDMPP-15EG	34	5	No	9
FPUF-10BDMPP-10EG	205	100	No	29
FPUF-15BDMPP-5EG	72	100	No	83

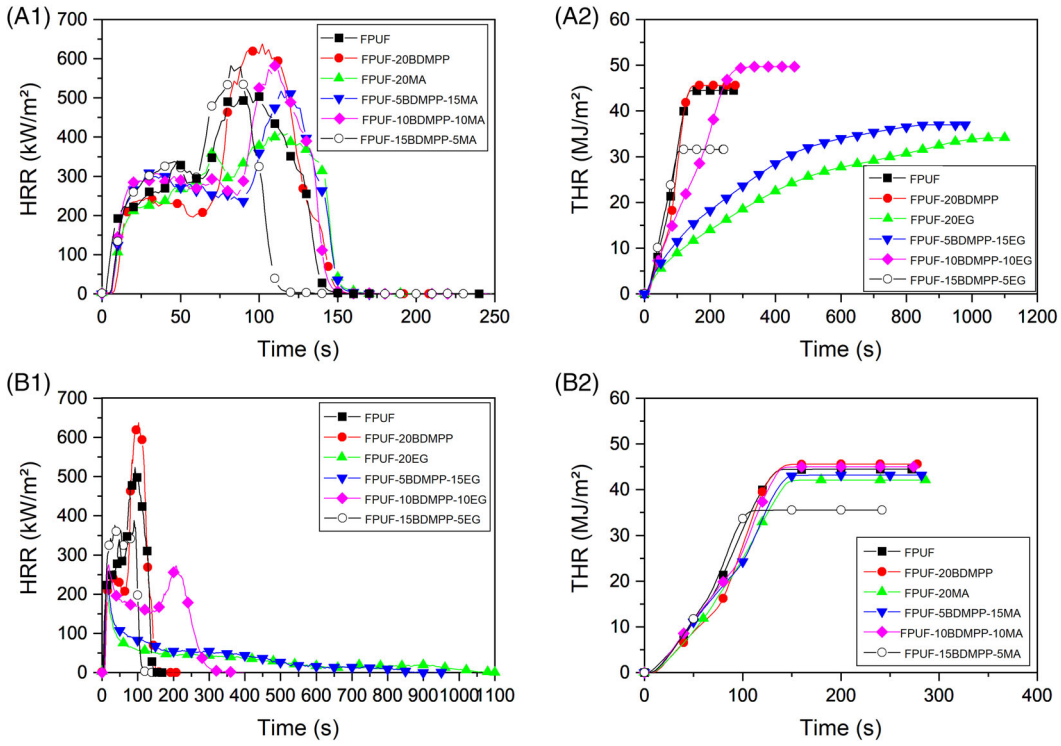

FIGURE 5 (A1) Heat release rate and (A2) total heat release rate of FPUF-BDMPP-MAs; (B1) heat release rate and (B2) total heat release rate of FPUF-BDMPP-EGs

TABLE 7 Table of cone calorimeter results

Sample	t_{ig} /s ± 1 s	PHRR /kW m^{-2}	THR /MJ m^{-2}	TML/g	Av. EHC/MJ kg^{-1}	Residue/ wt%	TSR /m^2 m^{-2}	MARHE/ kW m^{-2}
FPUF	6	503 ± 20	43.3 ± 0.1	16.9 ± 0.4	25.6 ± 0.6	0 ± 0.3	392 ± 4	320 ± 13
FPUF-20BDMPP	7	586 ± 52	42.3 ± 0.8	19.2 ± 0.8	22.0 ± 0.5	2.9 ± 1.9	946 ± 132	325 ± 7
FPUF-20MA	4	391 ± 20	40.3 ± 0.9	16.6 ± 0.2	24.3 ± 0.3	2.2 ± 0.8	299 ± 2	276 ± 11
FPUF-20EG	5	183 ± 19	16.2 ± 4.5	6.8 ± 1.7	23.6 ± 0.6	63.1 ± 7.7	52 ± 26	109 ± 10
FPUF-5BDMPP-15MA	5	523 ± 5	41.8 ± 0.9	18.2 ± 0.2	23.0 ± 0.1	4.6 ± 0.1	641 ± 22	310 ± 13
FPUF-10BDMPP-10MA	5	564 ± 18	43.1 ± 0.8	18.8 ± 0.2	22.9 ± 0.2	5.3 ± 0.4	757 ± 8	314 ± 8
FPUF-15BDMPP-5MA	4	559 ± 24	35.6 ± 0.4	16.1 ± 0.4	22.1 ± 0.3	4.7 ± 0.4	789 ± 36	328 ± 9
FPUF-5BDMPP-15EG	4	213 ± 27	22.4 ± 5.8	10.3 ± 2.0	21.4 ± 1.4	47.4 ± 4.7	204 ± 73	130 ± 17
FPUF-10BDMPP-10EG	5	252 ± 23	40.4 ± 8.0	18.3 ± 3.6	22.0 ± 0.1	12.3 ± 1.8	987 ± 291	173 ± 15
FPUF-15BDMPP-5EG	4	346 ± 42	31.6 ± 0.7	15.7 ± 0.2	20.1 ± 0.2	3.8 ± 1.5	998 ± 37	280 ± 28

Abbreviations: av, average; EHC, effective heat of combustion; MARHE, maximum average rate heat emission; PHRR, peak heat release rate; t_{ig}, time to ignition; THR, total heat release; TML, total mass loss; TSR, total smoke release.

concluded from the evolved gas analysis, radical scavenging occurred because phosphorus was released from BDMPP.[39] The presence of EG also showed a significant reduction in EHC. We hypothesize three contributions that could explain this phenomenon. EG created a protection layer, which caused incomplete pyrolysis in the second stage of burning. The second stage of burning generally corresponds mainly to the second step of pyrolysis. In PU the second stage of burning is usually characterized by a higher EHC.[18] Reducing the contribution of the second stage of burning results in a reduced contribution of the second decomposition step to the pyrolysis products, and thus reduces EHC. The second reason is the strongly increased charring in FPUF-20EG,which means that mainly graphitized carbon is stored with a higher effective heat of combustion than the PU. Thus, in the case of PU, increased charring goes along with emitting volatiles with a lower EHC than PU.[38] The last minor reason is that EG is treated with sulfuric acid as an intercalation reagent. During burning, the oxidation reaction of H_2SO_4 releases inert gases such as CO_2, SO_2, and,H_2O, which dilute the combustible gas.[16,40,41] Compared to other flame retardants, MA only shows a small effect on EHC through some fuel dilution. The FPUFs with the combination of BDMPP and EG,

especially FPUF-15BDMPP-5EG (20.1 MJ kg^{-1}), exhibit significant reduction in EHC values. The EHC of FPUF-15BDMPP-5EG reduced more than 21% compared with that of FPUF. As can be seen from this phenomenon, there was a synergistic effect between BDMPP and EG in the gas phase.

The pHRR of FPUF-20MA was reduced by 22% because MA acts as a heat sink to increase the heat capacity of the system and limits the increase in surface temperature of FPUF. Hence, MA reduces the generation rate of volatile fuel and decreases the pHRR effectively.[42] Considering Figure 5(A2), the burning time and THR of FPUF-15BDMPP-5MA are reduced significantly compared to those of either FPUF-20BDMPP or FPUF-20MA. Therefore, a synergistic effect was observed between 15-phr BDMPP and 5-phr MA in FPUF.

Even with the low loadings of EG presented in the system, the shape of the HRR curve was clearly changed. The addition of higher EG content led to a profound reduction in the PHRR, as the peaks became significantly smaller, with the curves much flatter. EG provides for significant charring, leading to the formation of a thermal insulating barrier which slows down the transfer of heat and mass within the pyrolysis zone for further decomposition in the condensed phase. The expanded graphite increases the thickness of the char layer to prolong the time of burning. This can be explained in detail with the cone calorimeter data

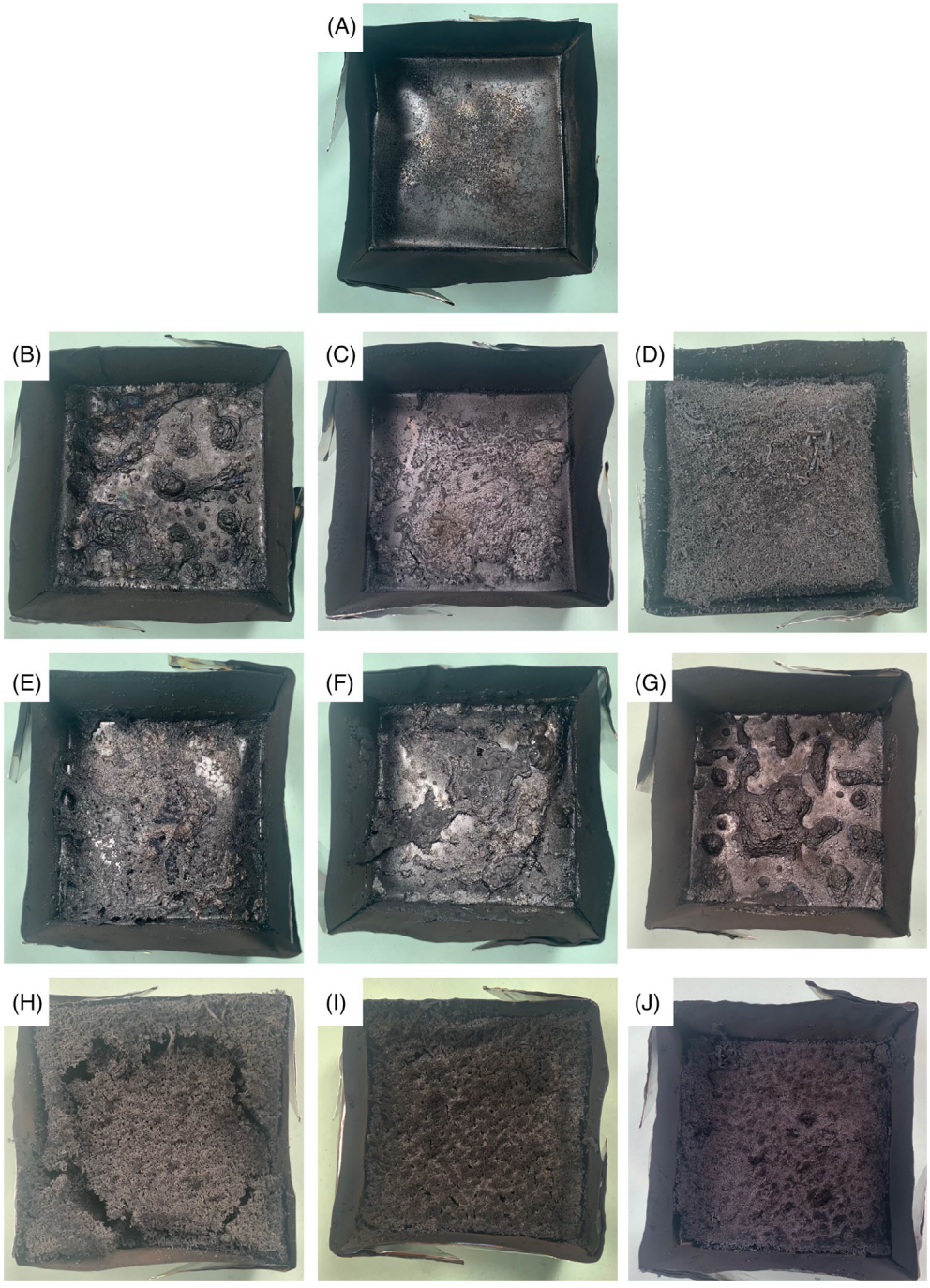

FIGURE 6 Fire residue images of (A) FPUF, (B) FPUF-20BDMPP, (C) FPUF-20MA, (D) FPUF-20EG, (E) FPUF-5BDMPP-15MA, (F) FPUF-10BDMPP-10MA, (G) FPUF-15BDMPP-5MA, (H) FPUF-5BDMPP-15EG, (I) FPUF-10BDMPP-10EG, (J) FPUF-15BDMPP-5EG

and the fire behavior of FPUF-20EG. At the beginning of the curve, the polymer matrix was under heat exposure, and thus the HRR increased swiftly. After the first sharp peak, the HRR dropped quickly because the EG expanded underheat, and acted as an excellent protective layer to save the material underneath.

THR is a measure of the entire amount of heat energy evolved during the burning time of the material. The THR decreased drastically from 43.3 MJm^{-2} for the non-flame retarded foam to 16.2 MJ m^{-2} for FPUF-20EG. The reduced value indicates that the expanded graphite formed protective layer, providing an excellent shielding

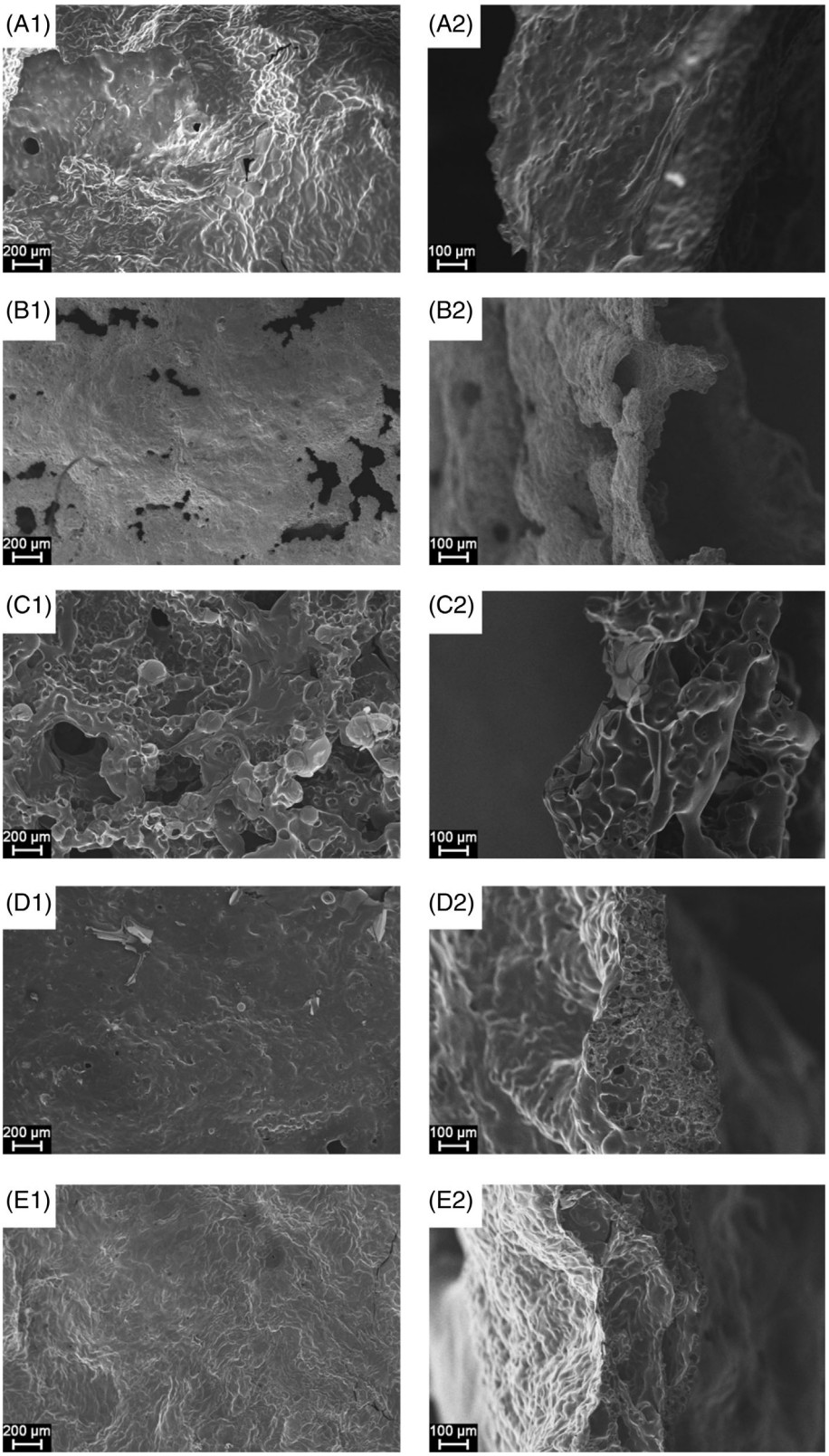

FIGURE 7 (A1) Surface and (A2) side view of FPUF-20BDMPP; (B1) surface and (B2) side view of FPUF-20MA; (C1) surface and (C2) side view of FPUF-5BDMPP-15MA; (D1) surface and (D2) side view of FPUF-10BDMPP-10MA; (E1) surface and (E2) side view of FPUF-15BDMPP-5MA

effect to the material underneath and leading to incomplete combustion. As combined with the results from the EHC and the yield of residue, the charring effect of EG in the condensed phase caused the major reduction in THR.

MARHE is one of the fire hazard indices of developing fires under a real-scale fire scenario. This is used to determine the combustibility of a material. The MARHE value of FPUF-20EG is reduced remarkably, to almost onethird that of the non-flame retarded foam. The FPUF-BDMPP-MAs show no changes in MARHE, but the FPUF-BDMPP-EGs lowered the value significantly. Based on the results for MARHE, EG is apparently an effective additive to reduce the MARHE.

The TSR of FPUF-20BDMPP is 946 m^2 m^{-2}, which indicates that BDMPP generates a large amount of smoke. This value is nearly 2.5 times that of FPUF. FPUF-20MA and FPUF-20EG greatly suppressed the smoke. Melamine acts as an inert diluent in the gas phase to reduce smoke emission.[43] D. Price et al. showed a chemical interaction between the melamine and the isocyanate at temperaturesover 250°C through the reaction between —NH_2 and —NCO. This interaction suppressed the smoke produced from isocyanate.[42] The great charring ability of EG produced a compact carbonaceous char that could limit the release of aromatic hydrocarbons to form smoke from the condensed phase into the gas phase.

3.6 | Fire residues

Figure 6 shows the images for the char residue of FUPFs after cone calorimeter measurement. FPUF in Figure 6A was consumed completely after burning and almost no residue remained. Figure 6B, C,E, F,G display a thin layer of fragile inorganic residue that remained in the aluminum foil tray. The micrographs of the FPUFs with EG (Figure 6D, H, I, J) show that the char layer formed during burning provided a thermal insulation barrier to protect the inner polymer matrix and to prevent further decomposition. According to Figure 6H, I, J, the integrity of expanded graphite residue was retained due to the presence of a sufficient amount of BDMPP.[44] The gluing effect by the phosphorous compound reinforced the integrity and continuity of the char layers, resulting in an enhanced barrier formed in the condensed phase.[32,45]

Figure 7 shows SEM images of the fire residue of FPUF-BDMPP20, FPUF-20MA, FPUF-5BDMPP-15MA, FPUF-10BDMPP-10MA, and FPUF-15BDMPP-5MA. FPUF-20BDMPP produced an intact and dense char residue which acted as a protective layer to the materials underneath during burning. FPUF-20MA resulted in a thin, layered residue with more holes on the surface. When 5-phr of MA from FPUF-20MA was replaced with 5-phr BDMPP, fire residue changed significantly on the surface and in the crosssection. Interestingly, FPUF-5BDMPP-15MA has a bumpy surface with a random size of holes and bubbles. Both FPUF-10BDMPP-10MA and FPUF-15BDMPP-5MA show a closed char surface. FPUF-10BDMPP-10MA exhibits a layer of tiny, compacted bubbles in its crosssection, while FPUF-15BDMPP-5MA consists of multiple layers with small bubbles and holes. The layered structure exhibited excellent protection against fire during burning.[46] Hence, the THR of FPUF-15BDMPP-5MA was significantly reduced.

4 | CONCLUSIONS

In this work, a set of flame retarded FPUF samples was prepared to understand the interaction between BDMPP and MA/EG. In each flame retarded sample, the total amount of additives was 20 phr. From the result of LOI and UL 94 HBF tests, all flame retarded samples showed reduced flammability and a lower burning rate. In the systems with a single flame retardant, both 20-phr BDMPP and 20-phr EG enhanced flame retardancy in the gas phase. 20-phr MA and 20-phr EG reduced the pHRR significantly. EG is a great smoke suppressant, according to the result of TSR from the cone calorimeter. FPUF-20EG produced only 13% of the amount of smoke released by FPUF. FPUF-20BDMPP and FPUF-20EG exhibited high char yield after a pyrolysis process. As to the systems with dual flame retardants, the overall flame retardancy of FPUF-BDMPP-EGs was better than that of FPUF-BDMPP-MAs. The synergistic effect between BDMPP and EG, mainly due to BDMPP contributing gluing effect to expanded graphite, improved the char yield and stopped dripping. Among FPUF-BDMPP-EGs, FPUF-5BDMPP-15EG showed the best flame retardancy properties according to the LOI value and the burning rate in UL 94 HBF. Self-extinguishing behavior was also observed for FPUF-5BDMPP-15EG from the UL 94 HBF test.

In summary, the thermal pyrolysis and fire performance indicate that the combination of BDMPP and EG actively improves the fire behavior of PFUF by synergistic effects in the gas and condensed phases.

ACKNOWLEDGEMENTS

The authors appreciate the contribution of the mechanical tests from D. Schulze. This project was financed by the DFG (Deutsche Forschungsgemeinschaft) (SCHA 730/19-1) and the NSFC (National Natural Science Foundation of China) (51761135113).

Open access funding enabled and organized by Projekt DEAL.

CONFLICT OF INTEREST

The authors declare no potential conflict of interest.

DATA AVAILABILITY STATEMENT

The data that support the findings of this study are available from the corresponding author upon reasonable request.

ORCID

Yuan Hu https://orcid.org/0000-0003-0753-5430
Bernhard Schartel https://orcid.org/0000-0001-5726-9754

REFERENCES

1. Jiang L, Ren Z, Zhao W, Liu W, Liu H, Zhu C. Synthesis and structure/properties characterizations of four polyurethane model hard segments. *R Soc Open Sci*. 2018;5(7):180536.

2. Günther M, Levchik SV, Schartel B. Bubbles and collapses: fire phenomena of flame-retarded flexible polyurethane foams. *Polym Adv Technol*. 2020;31(10):2185-2198.
3. Günther M, Lorenzetti A, Schartel B. Fire phenomena of rigid polyurethane foams. *Polymers*. 2018;10(10):1166.
4. Günther M, Lorenzetti A, Schartel B. From cells to residues: flame-retarded rigid polyurethane foams. *Combust Sci Technol*. 2020;192(12):2209-2237.
5. Lefebvre J, Le Bras M, Bastin B, Paleja R, Delobel R. Flexible polyurethane foams: flammability. *J Fire Sci*. 2003;21(5):343-367.
6. Weil ED, Levchik SV. *Flame Retardants for Plastics and Textiles Practical Applications*. Hanser Publishers; 2016.
7. Lorenzetti A, Besco S, Hrelja D, et al. Phosphinates and layered silicates in charring polymers: the flame retardancy action in polyurethane foams. *Polym Degrad Stabil*. 2013;98(11):2366-2374.
8. Schartel B, Wilkie CA, Camino G. Recommendations on the scientific approach to polymer flame retardancy: part 2 Concepts. *J Fire Sci*. 2017;35(1):3-20.
9. Wilke A, Langfeld K, Ulmer B, et al. Halogen-free multicomponent flame retardant thermoplastic styrene-ethylene-butylene-styrene elastomers based on ammonium polyphosphate-expandable graphite synergy. *Ind Eng Chem Res*. 2017;56(29):8251-8263.
10. Rao W-H, Liao W, Wang H, Zhao H-B, Wang Y-Z. Flame-retardant and smoke-suppressant flexible polyurethane foams based on reactive phosphorus-containing polyol and expandable graphite. *J Hazard Mater*. 2018;360:651-660.
11. Feng F-F, Qian L-J. The flame retardant behaviors and synergistic effect of expandable graphite and dimethyl Methylphosphonate in rigid polyurethane foams. *Polym Compos*. 2014;35(2):301-309.
12. Yuan Y, Yang H, Yu B, et al. Phosphorus and nitrogen-containing polyols: synergistic effect on the thermal property and flame Retardancy of rigid polyurethane foam composites. *Ind Eng Chem Res*. 2016;55(41):10813-10822.
13. Gaan S, Sun G, Hutches K, Engelhard M-H. Effect of nitrogen additives on flame retardant action of tributyl phosphate: phosphorus-nitrogen synergism. *Polym Degrad Stabil*. 2008;93(1):99-108.
14. Zhou F, Zhang T, Zou B, et al. Synthesis of a novel liquid phosphorus-containing flame retardant for flexible polyurethane foam: combustion behaviors and thermal properties. *Polym Degrad Stabil*. 2020;171:109029.
15. Zhang L-Q, Zhang M, Zhou Y-H, Hu L-H. The study of mechanical behavior and flame retardancy of castor oil phosphate-based rigid polyurethane foam composites containing expanded graphite and triethyl phosphate. *Polym Degrad Stabil*. 2013;98(12):2784-2794.
16. Lorenzetti A, Dittrich B, Schartel B, Roso M, Modesti M. Expandable graphite in polyurethane foams: the effect of expansion volume and intercalants on flame retardancy. *J Appl Polym Sci*. 2017;134(31):45173.
17. König A, Fehrenbacher U, Hirth T, Kroke E. Flexible polyurethane foam with the flame-retardant melamine. *J Cell Plast*. 2008;44(6):469-480.
18. Sut A, Metzsch-Zilligen E, Grosshauser M, Pfaendner R, Schartel B. Rapid mass calorimeter as a high-throughput screening method for the development of flame-retarded TPU. *Polym Degrad Stabil*. 2018;156:43-58.
19. Ugarte L, Saralegi A, Fernandez R, Martin L, Corcuera MA, Eceiza A. Flexible polyurethane foams based on 100% renewably sourced polyols. *Ind Crop Prod*. 2014;62:545-551.
20. Yang H-Y, Liu H-Y, Jiang Y-P, Chen M-F, Wan C-J. Density effect on flame Retardancy, thermal degradation, and combustibility of rigid polyurethane foam modified by expandable graphite or ammonium polyphosphate. *Polymers*. 2019;11(4):668.
21. Wendels S, Chavez T, Bonnet M, Salmeia KA, Gaan S. Recent developments in organophosphorus flame retardants containing P-C bond and their applications. *Materials*. 2017;10(7):784.
22. Ming G, Chen S, Sun Y-J, Wang Y-X. Flame Retardancy and thermal properties of flexible polyurethane foam containing expanded graphite. *Combust Sci Technol*. 2017;189(5):793-805.
23. Wang WJ, Dong K-H-Q, Zhu N, et al. Synergistic effect of aluminum hydroxide and expandable graphite on the flame Retardancy of Polyisocyanurate-polyurethane foams. *J Appl Polym Sci*. 2014;131(4):39936.
24. Yang S, Wang J, Huo S-Q, Wang M, Wang J-P, Zhang B. Synergistic flame-retardant effect of expandable graphite and phosphorus-containing compounds for epoxy resin: strong bonding of different carbon residues. *Polym Degrad Stabil*. 2016;128:89-98.
25. Luo F-B, Wu K, Lu M-G. Enhanced thermal stability and flame retardancy of polyurethane foam composites with polybenzoxazine modified ammonium polyphosphates. *RSC Adv*. 2016;6(16):13418-13425.
26. Liu W, Tang Y, Li F, Ge X-G, Zhang Z-J. TG-FTIR characterization of flame retardant polyurethane foams materials. *Iop Conf Ser-Mat Sci*. 2016;137:012033.
27. Chen D-M, Zhao Y-P, Yan J-J, Chen L, Dong Z-Z, Fu W-G. Preparation and properties of halogen-free flame retardant polyurethane foams. *Adv Mater Res-Switz*. 2012;418–420:540-543.
28. Lin F, Lin H, Ke J, Liu J, Bai X, Chen D. Preparation of reactive and additive flame retardant with different oxidation state of phosphorus on the thermal and flammability of thermoplastic polyurethane. *Compos Mater*. 2019;3(2):43-53.
29. Zhu H, Xu S-A. Preparation of flame-retardant rigid polyurethane foams by combining modified melamine-formaldehyde resin and phosphorus flame retardants. *ACS Omega*. 2020;5(17):9658-9667.
30. Ravey M, Pearce EM. Flexible polyurethane foam. I. Thermal decomposition of a polyether-based, water-blown commerical type of flexible polyurethane foam. *J Appl Polym Sci*. 1997;63(1):47-74.
31. Lewin M. Synergistic and catalytic effects in flame retardancy of polymeric materials—an overview. *J Fire Sci*. 1999;17(1):3-19.
32. Liu D-Y, Zhao B, Wang J-S, Liu P-W, Liu Y-Q. Flame retardation and thermal stability of novel phosphoramide/expandable graphite in rigid polyurethane foam. *J Appl Polym Sci*. 2018;135(27):46434.
33. Hu Y, Zhou Z, Li S, Yang D, Zhang S, Hou Y. Flame retarded rigid polyurethane foams composites modified by aluminum diethylphosphinate and expanded graphite. *Front Mater*. 2021;7:471.
34. Sut A, Metzsch-Zilligen E, Grosshauser M, Pfaendner R, Schartel B. Synergy between melamine cyanurate, melamine polyphosphate and aluminum diethylphosphinate in flame retarded thermoplastic polyurethane. *Polym Test*. 2019;74:196-204.
35. Rabe S, Chuenban Y, Schartel B. Exploring the modes of action of phosphorus-based flame retardants in polymeric systems. *Materials*. 2017;10(5):455.
36. Baguian AF, Ouiminga SK, Longuet C, et al. Influence of density on foam collapse under burning. *Polymers*. 2021;13(1):13.
37. Kramer RH, Zammarano M, Linteris GT, Gedde UW, Gilman JW. Heat release and structural collapse of flexible polyurethane foam. *Polym Degrad Stabil*. 2010;95(6):1115-1122.
38. Schartel B. Phosphorus-based flame Retardancy mechanisms-old hat or a starting point for future development? *Materials*. 2010;3(10):4710-4745.
39. Lorenzetti A, Modesti M, Gallo E, Schartel B, Besco S, Roso M. Synthesis of phosphinated polyurethane foams with improved fire behavior. *Polm Degrad Stabil*. 2012;97(11):2364-2369.
40. Modesti M, Lorenzetti A, Simioni F, Camino G. Expandable graphite as an intumescent flame retardant in polyisocyanurate-polyurethane foams. *Polym Degrad Stabil*. 2002;77(2):195-202.
41. Camino G, Duquesne S, Delobel R, Eling B, Lindsay C, Roels T. Mechanism of expandable graphite fire retardant action in polyurethanes. *Abstr Pap Am Chem S*. 2000;220:U333-U334.
42. Price D, Liu Y, Milnes GJ, Hull R, Kandola BK, Horrocks AR. An investigation into the mechanism of flame retardancy and smoke

suppression by melamine in flexible polyurethane foam. *Fire Mater*. 2002;26(4–5):201-206.
43. Xu Q-W, Zhai H-M, Wang G-J. Mechanism of smoke suppression by melamine in rigid polyurethane foam. *Fire Mater*. 2015;39(3):271-282.
44. Gómez-Fernández S, Günther M, Schartel B, Corcuera MA, Eceiza A. Impact of the combined use of layered double hydroxides, lignin and phosphorous polyol on the fire behavior of flexible polyurethane foams. *Ind Crop Prod*. 2018;125:346-359.
45. Li J, Mo X-H, Li Y, Zou H-W, Liang M, Chen Y. Influence of expandable graphite particle size on the synergy flame retardant property between expandable graphite and ammonium polyphosphate in semi-rigid polyurethane foam. *Polym Bull*. 2018;75(11):5287-5304.
46. Rao W-H, Hu Z-Y, Xu H-X, et al. Flame-retardant flexible polyurethane foams with highly efficient melamine salt. *Ind Eng Chem Res*. 2017;56(25):7112-7119.

How to cite this article: Chan YY, Ma C, Zhou F, Hu Y, Schartel B. A liquid phosphorous flame retardant combined with expandable graphite or melamine in flexible polyurethane foam. *Polym Adv Technol*. 2022;33(1):326-339. doi: 10.1002/pat.5519